K-dimensional trio coherent states

2004 J. Phys. A: Math. Gen. 37 11017

(http://iopscience.iop.org/0305-4470/37/45/019)

INSTITUTE OF PHYSICS PUBLISHING JOURNAL OF PHYSICS A: MATHEMATICAL AND GENERAL

J. Phys. A: Math. Gen. **37** (2004) 11017–11036 PII: S0305-4470(04)78583-2

K-dimensional trio coherent states

Hyo Seok Yi[1], **Ba An Nguyen**[2,3] **and Jaewan Kim**[2]

[1] Department of Physics, Korea Advanced Institute of Science and Technology, 373-1 Guseong-dong, Yuseong-gu, Daejeon 305-701, Korea
[2] School of Computational Sciences, Korea Institute for Advanced Study, 207-43 Cheongryangni 2-dong, Dongdaemun-gu, Seoul 130-722, Korea

E-mail: hsyi@muon.kaist.ac.kr, nbaan@kias.re.kr and jaewan@kias.re.kr

Received 29 March 2004
Published 28 October 2004
Online at stacks.iop.org/JPhysA/37/11017
doi:10.1088/0305-4470/37/45/019

Abstract

We introduce a novel class of higher-order, three-mode states called *K*-dimensional trio coherent states. We study their mathematical properties and prove that they form a complete set in a truncated Fock space. We also study their physical content by explicitly showing that they exhibit nonclassical features such as oscillatory number distribution, sub-Poissonian statistics, Cauchy–Schwarz inequality violation and phase-space quantum interferences. Finally, we propose an experimental scheme to realize the state with $K = 2$ in the quantized vibronic motion of a trapped ion.

PACS numbers: 42.50.−p, 42.50.Vk, 32.80.Pj

(Some figures in this article are in colour only in the electronic version.)

1. Introduction

Higher-order effects as well as the multimode nature of quantum states play a significant role in various physical applications. For instance, while multimode entangled states serve as necessary resources in a multiuser quantum communication network (see, e.g., [1–3]), higher-order character gives rise to simultaneous squeezing in several directions [4–6] or to enhancement of antibunching [7], etc. Here we deal with states that are higher-order and three-mode.

The motivation for studying such states is twofold. Firstly, is the academic motivation since we shall go on a route similar to those from one-dimensional (1D) single-mode (two-mode) coherent states to *K*-dimensional single-mode [8–14] (two-mode [15–18]) coherent states. Our study concerns the case of three modes thus generalizing the previously existing works. Our three-mode states are intrinsically nonclassical (see [19] for a comprehensive review).

[3] Author to whom correspondence should be addressed.

It is worth mentioning here that a number of nonclassical states are intimately linked with a symmetry group. But this does not compulsorily hold for all nonclassical states. For example, the N-mode sum-squeezed states [20, 21] are always (i.e., for any $N \geqslant 2$) connected with the $su(1,1)$ Lie algebra. Yet, the operators characterizing the N-mode difference-squeezed state [20, 22] forms a representation of the $su(2)$ Lie algebra only for $N = 2$, not for $N \geqslant 3$ [23]. The states we are going to study in this paper have no relation to a symmetry group. Secondly, the practical motivation could also be foreseen. As will be shown, a K-dimensional state is in fact a quantum superposition of K massive distinguishable substates. Such superpositions not only help in a deeper understanding of the physics world both from the quantum and classical points of view, but they may also serve as resources for quantum computation and quantum information processing. Moreover, our three-mode states are *naturally* entangled and, as such, they potentially promise wide applications. In this connection we notice that pair coherent states (PCS) [24], which are of two-mode entangled character, have been found useful in testing fundamental concepts of physics [25–28] as well as in accomplishing quantum teleportation [29, 30]. We therefore believe that there should be tasks (say, with the participation of three parties such as Fredkin or Toffoli gates and so on) which cannot be performed by single- or two-mode states but can be performed by three-mode ones such as ours.

The states of interest are defined as the eigenstates of the operator $(\hat{a}\hat{b}\hat{c})^K$, with K a positive integer and $\hat{a}$ $(\hat{b}, \hat{c})$ the boson annihilation operator of mode a (b, c), subject to the conditions that they are also the eigenstates of the operators $\widehat{P} = \hat{b}^\dagger\hat{b} - \hat{c}^\dagger\hat{c}$ and $\widehat{Q} = \hat{a}^\dagger\hat{a} - \hat{c}^\dagger\hat{c}$ corresponding to the differences of the number of quanta in the three modes. It is noted that the operators $\hat{a}$, $\hat{b}$ and $\hat{c}$ commute with each other. Denoting the state by $|\xi, p, q\rangle_K$, the following three equations must be simultaneously satisfied:

$$(\hat{a}\hat{b}\hat{c})^K|\xi, p, q\rangle_K = \xi^K|\xi, p, q\rangle_K, \tag{1}$$

$$\widehat{P}|\xi, p, q\rangle_K = p|\xi, p, q\rangle_K, \tag{2}$$

$$\widehat{Q}|\xi, p, q\rangle_K = q|\xi, p, q\rangle_K, \tag{3}$$

where $\xi = r\exp(\mathrm{i}\varphi) \in \mathcal{C}$ and p, q are referred to as 'charges' [31, 32] which, without loss of generality, are assumed to be non-negative. Equations (1)–(3) signify that a superposition of three-mode Fock states in the form

$$|\xi, p, q\rangle_K = \sum_{n=0}^{\infty} c_n|n+q\rangle_a|n+p\rangle_b|n\rangle_c \tag{4}$$

is a solution provided the coefficients c_n obey the constraint

$$c_{n+K} = \sqrt{\frac{(n+q)!(n+p)!n!}{(n+q+K)!(n+p+K)!(n+K)!}}\,\xi^K c_n. \tag{5}$$

This constraint forms K independent strings $\{s_0, s_1, \ldots, s_{K-1}\}$ where each of s_j consists of an infinite number of related coefficients $s_j = \{c_j, c_{j+K}, c_{j+2K}, \ldots\}$ with c_j being the representative of the s_j-string. The states $|\xi, p, q\rangle_K$ are therefore highly degenerate since the representatives c_0, $c_1, \ldots, c_{K-1}$ remain arbitrary. We now impose conditions on the representative c_j so that a state $|\xi, p, q\rangle_{Kj}$ associated with the coefficients taken from the s_j-string is normalized to unity. (Note that the subscript Kj should not be conceived as a single index; it refers to two separate integers K and j.) Then, each state $|\xi, p, q\rangle_{Kj}$ with a fixed

$j \in [0, K-1]$ has the following explicit Fock expansion:

$$|\xi, p, q\rangle_{Kj} = N_{Kj}(r^2, p, q) \sum_{n=0}^{\infty} \frac{\xi^{Kn+j}}{\sqrt{\rho_{pq0}(Kn+j)}} |Kn+j+q\rangle_a |Kn+j+p\rangle_b |Kn+j\rangle_c, \quad (6)$$

where

$$\rho_{pq0}(Kn+j) = (Kn+j+p)!(Kn+j+q)!(Kn+j)! \quad (7)$$

and

$$N_{Kj}(x, p, q) = \left(\sum_{m=0}^{\infty} \frac{x^{Km+j}}{\rho_{pq0}(Km+j)} \right)^{-1/2} \quad (8)$$

is the normalization coefficient. Since the overlap between states $|\xi, p, q\rangle_{Kj}$ and $|\xi', p', q'\rangle_{Kj'}$ is determined by

$$_{Kj'}\langle \xi', p', q' \mid \xi, p, q\rangle_{Kj} = \delta_{jj'}\delta_{pp'}\delta_{qq'} \frac{N_{Kj}(\xi'^*, p, q) N_{Kj}(\xi, p, q)}{N_{Kj}^2(\sqrt{\xi'^*\xi}, p, q)}, \quad (9)$$

it follows that the normalized states $|\xi, p, q\rangle_{Kj}$ are orthogonal with respect to j, p, q but nonorthogonal with respect to ξ. It is worth emphasizing that for a given K there are K states $|\xi, p, q\rangle_{Kj}$ ($j = 0, 1, \ldots, K-1$), each of which is a three-mode entangled state. In other words, the eigenvalue set $\{\xi^K, p, q\}$ is K-degenerate corresponding to K linearly independent eigenstates $|\xi, p, q\rangle_{Kj}$. We call them K-dimensional trio coherent states (KTCSs) because the dimension of the space spanned by these states is K even though each of them is embedded in a vector space of infinite dimension characterized by the complex variable ξ. In the same spirit, multidimensional entangled coherent states have also been investigated recently in [33] where it is proved that they are necessary for teleportation of quantum states of a particular kind. When $K = 1$ the KTCS reduces to the trio coherent state (TCS) introduced in [34] which is a generalization of the PCS [24]. So, in what follows, when KTCSs are quoted it is implied $K > 1$.

In the next part of this paper we first expose the mathematical properties of the KTCSs including proof of their (over)completeness. Physical properties are then studied showing that KTCSs are inherently nonclassical. Finally, we propose an experimental scheme to produce a KTCS in the vibrational motion of the centre-of-mass of an ion trapped in real space by a 3D harmonic potential.

2. Mathematical properties

States $|\xi, p, q\rangle_{Kj}$ with different j can be transformed from one to another by a 'rotation' operator $\widehat{R}_{Klm}(\xi, p, q)$ defined by

$$\widehat{R}_{Klm}(\xi, p, q) = \frac{N_{Kl}(r^2, p, q)}{N_{Km}(r^2, p, q)} \xi^{-[m-l]_K} (\hat{a}\hat{b}\hat{c})^{[m-l]_K}, \quad (10)$$

where $[x]_K = x$ if $x \geqslant 0$ and $[x]_K = x + K$ if $x < 0$. That is, for any $l, m \in [0, K-1]$,

$$|\xi, p, q\rangle_{Kl} = \widehat{R}_{Klm}(\xi, p, q) |\xi, p, q\rangle_{Km}. \quad (11)$$

Another important property is: any KTCS can be expressed as a superposition of K phase-correlated TCSs. Namely,

$$|\xi, p, q\rangle_{Kj} = \frac{N_{Kj}(r^2, p, q)}{KN(r^2, p, q)} \sum_{j'=0}^{K-1} \exp\left(-\frac{2\pi \mathrm{i}}{K} jj'\right) |\xi_{Kj'}, p, q\rangle, \quad (12)$$

where $|\xi, p, q\rangle \equiv |\xi, p, q\rangle_{10}$, $N(r^2, p, q) \equiv N_{10}(r^2, p, q)$ and

$$\xi_{Kj} = \xi \exp\left(\frac{2\pi \mathrm{i} j}{K}\right). \tag{13}$$

Expansion (12) can be straightforwardly verified by virtue of the identities $\sum_{m=0}^{K-1} \exp[2\pi \mathrm{i}(l - l')m/K] \equiv K\delta_{ll'}$ and $\sum_{m=0}^{\infty} X_m|m\rangle \equiv \sum_{l=0}^{K-1}\sum_{n=0}^{\infty} X_{nK+l}|nK + l\rangle$. It can be noted, due to equation (13), that the TCSs superposing a KTCS are evenly distributed on a circle of radius r in the phase space. The inverse transformation of (12) is

$$|\xi_{Kj}, p, q\rangle = N(r^2, p, q) \sum_{j'=0}^{K-1} \frac{\exp[(2\pi \mathrm{i}/K) jj']}{N_{Kj'}(r^2, p, q)} |\xi, p, q\rangle_{Kj'}. \tag{14}$$

Alternatively, making a change $\{\xi_{Kj} \equiv \xi \exp(2\pi \mathrm{i} j/K) \to \chi, \xi \to \chi \exp(-2\pi \mathrm{i} j/K)\}$ in (14) and taking into account the identity

$$|\chi \exp(-2\pi \mathrm{i} j/K), p, q\rangle_{Kj'} \equiv \exp(-2\pi \mathrm{i} jj'/K)|\chi, p, q\rangle_{Kj'} \tag{15}$$

which can be easily checked by use of the Fock representation (6) on both sides of (15), we can cast (14) into a simpler but more convenient form (after changing χ back to ξ) as

$$|\xi, p, q\rangle = N(r^2, p, q) \sum_{j=0}^{K-1} \frac{|\xi, p, q\rangle_{Kj}}{N_{Kj}(r^2, p, q)}. \tag{16}$$

More interestingly, it turns out that KTCSs of any two different dimensions are also related to each other. A hint to establish such a relation is first using (12) to express a KTCS with a given K in terms of TCSs and then applying (16) to get the TCSs back in terms of K′TCSs with a different K' (generally $K' \neq K$). As a result, we arrive at

$$|\xi, p, q\rangle_{Kj} = \frac{N_{Kj}(x, p, q)}{K} \sum_{j'=0}^{K'-1} \sum_{j''=0}^{K-1} \frac{\exp\left(-\frac{2\pi \mathrm{i}}{K} jj''\right)}{N_{K'j'}(x, p, q)} |\xi_{Kj''}, p, q\rangle_{K'j'}. \tag{17}$$

The transformation (17) is most general in the sense that it recovers (12) when $K' = 1$, $j' = 0$ and (16) when $K = 1$, $j = 0$. In the special case, when $K' = K$, the rhs of (17) becomes nothing other than its lhs, as it should be.

In terms of the usual single-mode coherent state

$$|\eta) \equiv \exp(-|\eta|^2/2) \sum_{n=0}^{\infty} \frac{\eta^n}{\sqrt{n!}} |n\rangle, \tag{18}$$

the following expansion holds in general:

$$|\xi, p, q\rangle_{Kj} = N_{Kj}(r^2, p, q) \int \frac{\alpha^{*q}\, \mathrm{d}^2\alpha}{\pi} \int \frac{\beta^{*p}\, \mathrm{d}^2\beta}{\pi} \int \frac{\mathrm{d}^2\gamma}{\pi} N_{Kj}^{-2}(\xi\alpha^*\beta^*\gamma^*, p, q)$$
$$\times \exp[-(|\alpha|^2 + |\beta|^2 + |\gamma|^2)/2]|\alpha)_a|\beta)_b|\gamma)_c \tag{19}$$

because of the completeness of the coherent state. In particular, however, a formula via three phase-correlated coherent states whose amplitudes α, β and γ satisfy the equality $\alpha\beta\gamma = \xi$

seems to be more useful. It can be written as

$$|\xi, p, q\rangle_{Kj} = \frac{1}{K} N_{Kj}(r^2, p, q) \exp[(|\alpha|^2 + |\beta|^2 + |\gamma|^2)/2]$$
$$\times \sum_{j'=0}^{K-1} \frac{\exp\left(-\frac{2\pi \mathrm{i}}{K} jj'\right)}{\alpha_{Kj'}^q \beta_{Kj'}^p} \int_0^{2\pi} \frac{\mathrm{d}\theta}{2\pi} \int_0^{2\pi} \frac{\mathrm{d}\theta'}{2\pi} \exp[-\mathrm{i}(q\theta + p\theta')]$$
$$\times |\alpha_{Kj'} \exp(\mathrm{i}\theta))_a |\beta_{Kj'} \exp(\mathrm{i}\theta'))_b |\gamma_{Kj'} \exp[-\mathrm{i}(\theta + \theta')])_c. \tag{20}$$

In fact, when $K = 1$, $j = 0$ and $\alpha = \beta = \gamma = \xi^{1/3}$, formula (20) reduces to formula (1) in [35].

We now turn to the important issue of proving that the K states $|\xi, p, q\rangle_{Kj}$ ($j = 0, 1, \ldots, K-1$) form a complete set. As seen from (6), any state $|\xi, p, q\rangle_{Kj}$ spans the three-mode Fock space in which the q (p) first number states of mode a (b) with $n_a = 0, 1, \ldots, q-1$ ($n_b = 0, 1, \ldots, p-1$) are lacking. In such a truncated Fock space the unity operator has to be of the form (similar matter associated with single-mode photon-added coherent states can be found in [36])

$$\boldsymbol{I}_{p,q} = \sum_{n=0}^{\infty} |n+q\rangle_a |n+p\rangle_b |n\rangle_c \langle n|_b \langle n+p|_a \langle n+q| . \tag{21}$$

The resolution of unity of the KTCSs then amounts to the existence of a weight function $W_{Kj}(|\xi|^2, p, q)$ so as to fulfil the following completeness condition:

$$\sum_{j=0}^{K-1} \int \mathrm{d}^2\xi \, |\xi, p, q\rangle_{Kj} W_{Kj}(|\xi|^2, p, q)_{Kj} \langle \xi, p, q| = \mathbf{I}_{p,q}. \tag{22}$$

To solve for $W_{Kj}(|\xi|^2, p, q)$ we substitute $\xi = r\exp(\mathrm{i}\varphi)$ and (6) into (22) and integrate over φ. After the φ-integration the function $W_{Kj}(r^2, p, q)$ is looked for in the form

$$W_{Kj}(r^2, p, q) = \frac{\widetilde{W}(r^2, p, q, 0)}{\pi N_{Kj}^2(r^2, p, q)}, \tag{23}$$

where $\widetilde{W}(r^2, p, q, 0)$ is to be determined from the equation

$$\int_0^{\infty} \widetilde{W}(x, p, q, 0) x^n \, \mathrm{d}x = \rho_{pq0}(n), \qquad n = 0, 1, 2, \ldots, \infty. \tag{24}$$

This is the classical Stieltjes power-moment problem [37], with the set of nth moments $\rho_{pq0}(n)$ parametrized by $\{p, q, 0\}$. If n in equation (24) is extended to $s-1$ where $s \in \mathcal{C}$, then our problem can be formulated in terms of the Mellin and inverse Mellin transforms [38, 39] that have been extensively used in the context of various kinds of generalized coherent states [40–45]. Here, $\rho_{pq0}(s-1)$ is the Mellin transform, $\mathcal{M}[\widetilde{W}(x, p, q, 0); s]$, of $\widetilde{W}(x, p, q, 0)$, i.e.,

$$\rho_{pq0}(s-1) = \mathcal{M}[\widetilde{W}(x, p, q, 0); s] := \int_0^{\infty} \widetilde{W}(x, p, q, 0) x^{s-1} \, \mathrm{d}x \tag{25}$$

and $\widetilde{W}(x, p, q, 0)$ in turn is the inverse Mellin transform, $\mathcal{M}^{-1}[\rho_{pq0}(s-1); x]$, of $\rho_{pq0}(s-1)$, i.e.,

$$\widetilde{W}(x, p, q, 0) = \mathcal{M}^{-1}[\rho_{pq0}(s-1); x] := \frac{1}{2\pi \mathrm{i}} \int_{-\mathrm{i}\infty}^{\mathrm{i}\infty} \rho_{pq0}(s-1) x^{-s} \, \mathrm{d}s. \tag{26}$$

We know [44] that the solution of the simpler problem

$$\int_0^\infty \widetilde{W}(x,l)x^n\,\mathrm{d}x = \rho_l(n) = (n+l)! \tag{27}$$

is given by

$$\widetilde{W}(x,l) = \mathcal{M}^{-1}[\rho_l(s-1);x] = x^l\,\mathrm{e}^{-x}. \tag{28}$$

To make use of the known result (28), we apply twice the Parseval relation [38, 39] which we reformulate for our purpose here in the form

$$\mathcal{M}^{-1}[f(s-1)g(s-1);x] = \int_0^\infty \frac{\mathrm{d}t}{t}\mathcal{M}^{-1}[f(s-1);t]\mathcal{M}^{-1}\left[g(s-1);\frac{x}{t}\right]. \tag{29}$$

Now, by virtue of (26), (27) and (29), we have immediately

$$\begin{aligned}\widetilde{W}(x,p,q,0) &= \mathcal{M}^{-1}[\rho_{pq0}(s-1);x] \equiv \mathcal{M}^{-1}[\rho_p(s-1)\rho_q(s-1)\rho_0(s-1);x]\\ &= \int_0^\infty \frac{\mathrm{d}t}{t}\mathcal{M}^{-1}[\rho_p(s-1)\rho_q(s-1);t]\mathcal{M}^{-1}\left[\rho_0(s-1);\frac{x}{t}\right]\\ &= \int_0^\infty \frac{\mathrm{d}t}{t}\left[\int_0^\infty \frac{\mathrm{d}\tau}{\tau}\mathcal{M}^{-1}[\rho_p(s-1);\tau]\mathcal{M}^{-1}\left[\rho_q(s-1);\frac{t}{\tau}\right]\right]\\ &\quad\times\mathcal{M}^{-1}\left[\rho_0(s-1);\frac{x}{t}\right] = \int_0^\infty t^{q-1}\,\mathrm{e}^{-x/t}\left[\int_0^\infty \tau^{p-q-1}\,\mathrm{e}^{-\tau-t/\tau}\,\mathrm{d}\tau\right]\mathrm{d}t,\end{aligned} \tag{30}$$

where in the last step we made use of equation (28). Performing the τ-integration we finally arrive at

$$\widetilde{W}(x;\,p,q,0) = \int_0^\infty t^{-1+(p+q)/2}\,\mathrm{e}^{-x/t}K_{q-p}(2\sqrt{t})\,\mathrm{d}t, \tag{31}$$

where $K_n(t) = K_{-n}(t) = K_{|n|}(t)$ stands for the modified Bessel function of the second kind. There are two remarks to be made at this point as follows:

- The condition (22) is that of over-completeness rather than completeness. This is due to the nonorthogonality of KTCSs with respect to ξ and is explicitly reflected by the fact that any state $|\xi,p,q\rangle_{Kj}$ can be represented via the others as

$$|\xi,p,q\rangle_{Kj} = N_{Kj}(\xi,p,q)\int \mathrm{d}^2\xi'\,\frac{N_{Kj}(\xi'^*,p,q)W_{Kj}(|\xi'|^2,p,q)}{N_{Kj}^2(\sqrt{\xi'^*\xi},p,q)}|\xi',p,q\rangle_{Kj}. \tag{32}$$

- The solution (31) is not unique. According to Carleman's (sufficient) condition [46], our solution would be unique (non-unique) if the sum $S=\sum_{n=1}^\infty S_n$, with $S_n=[(Kn+j+q)!\times(Kn+j+p)!(Kn+j)!]^{-1/2n}$, diverges (converges). We now apply the logarithmic test [47] to examine the convergence of S. The logarithmic criterion says that if $T=\lim_{n\to\infty}\ln(S_n)/\ln(n) > -1\,(<-1)$ then S diverges (converges). To calculate T we rewrite S_n in terms of Gamma functions, $S_n=[\Gamma(Kn+j+q+1)\Gamma(Kn+j+p+1)\Gamma(Kn+j+1)]^{-1/2n}$, and then use Stirling's formula, $\Gamma(Kn+l)\approx\sqrt{2\pi}\,\exp(-Kn)(Kn)^{Kn}$, which is valid for large n and finite l ($l\ll n$). As a result, we obtain $\lim_{n\to\infty}\ln(S_n) = -3K\ln(n)/2$ and, hence, $T=-3K/2<-1$ for any positive integers K. This proves the non-uniqueness of our solution (31).

To end this section we recall from (6) that the KTCSs are normalized by the normalization coefficient $N_{Kj}(r^2, p, q)$ determined by (8). The states are also continuous in the variable ξ because $||\xi, p, q\rangle_{Kj} - |\xi', p, q\rangle_{Kj}|^2 = 2[1 - \mathrm{Re}({}_{Kj}\langle\xi', p, q|\xi, p, q\rangle_{Kj})]$ tends to vanish when $|\xi - \xi'| \to 0$, as is evident from (8) and (9). Furthermore, as follows from (23) and (31), the weight function $W_{Kj}(|\xi|^2, p, q)$ in (22) is guaranteed to be positive (owing to positivity of the Bessel function $K_n(t)$). Therefore, the minimal set of conditions [48, 49] required for an ensemble of states to be *coherent* is met for the KTCSs. That explains why '*coherent*' arises in naming the states $|\xi, p, q\rangle_{Kj}$ as '*K-dimensional trio coherent states*' for which '*coherent*' must be the family name and '*K-dimensional trio*' the first name.

3. Physical content

In this section we explore the physical content of the KTCSs. The probability of finding l (m, n) quanta of mode a (b, c) in state $|\xi, p, q\rangle_{Kj}$ is given by

$$P_{lmn}(\xi, p, q, K, j) = |{}_{Kj}\langle\xi, p, q|\, l, m, n\rangle_{abc}|^2 = P_n(\xi, p, q, K, j)\delta_{m,n+p}\delta_{l,n+q} \tag{33}$$

with

$$P_n(\xi, p, q, K, j) = \frac{r^{2n}N_{Kj}^2(r^2, p, q)I((n-j)/K)}{\rho_{pq0}(n)}, \tag{34}$$

where $I(x) = 1$ if x is an integer and $I(x) = 0$ if x is a non-integer. While the Kronecker symbols in (33) reveal the entanglement of the modes in state $|\xi, p, q\rangle_{Kj}$, the function $I\,((n-j)/K)$ in (34) indicates that for any $K > 1$ the number distribution of state $|\xi, p, q\rangle_{Kj}$ suffers an oscillation as shown in figure 1 in which the TCS is also plotted that does not oscillate at all.

Further information on inherent quantum statistics of state $|\xi, p, q\rangle_{Kj}$ can be obtained from the Mandel parameter M_x for mode x [50],

$$M_x = \frac{\langle\hat{n}_x^{(2)}\rangle - \langle\hat{n}_x\rangle^2}{\langle\hat{n}_x\rangle}, \tag{35}$$

where $\hat{n}_x = \hat{x}^\dagger\hat{x}$ with $\hat{x}$ the annihilation operator of mode x and the expectation value of the factorial moment of the number operator $\langle\hat{n}_x^{(l)}\rangle \equiv \langle\prod_{m=0}^{l-1}(\hat{n}_x - m)\rangle$ is derived for our KTCSs in the form

$$\langle\hat{n}_a^{(l)}\rangle = z^{l-q}N_{Kj}^2\frac{\mathrm{d}^l}{\mathrm{d}z^l}\left(\frac{z^q}{N_{Kj}^2}\right), \tag{36}$$

$$\langle\hat{n}_b^{(l)}\rangle = z^{l-p}N_{Kj}^2\frac{\mathrm{d}^l}{\mathrm{d}z^l}\left(\frac{z^p}{N_{Kj}^2}\right), \tag{37}$$

$$\langle\hat{n}_c^{(l)}\rangle = z^l N_{Kj}^2\frac{\mathrm{d}^l}{\mathrm{d}z^l}\left(\frac{1}{N_{Kj}^2}\right), \tag{38}$$

where $N_{Kj} \equiv N_{Kj}(z, p, q)$ and $z = r^2$. An evident factor that makes a difference between modes is the charges p, q. For $p = q = 0$ all three modes are 'identical'. For $p > q = 0$ $(q > p = 0)$ mode a (b) and mode c behave identically while however being distinct from mode b (a). For $p = q > 0$, modes a and b are similar while mode c is dissimilar. Only when $p \neq q$ and each

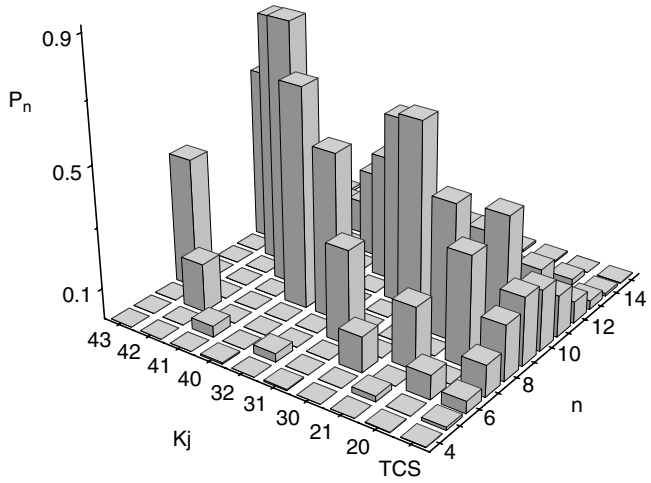

Figure 1. 3D bar plot showing oscillation of the number distribution, $P_n(\xi, p, q, K, j)$, for $r = 30$, $p = q = 0$ and different combinations of Kj. For comparison, the case of TCS which does not oscillate at all is also plotted.

of them acquires a positive integer are the three modes distinguishable from each other. The use of (36) in (35) yields explicitly

$$M_a = \frac{2z^2(N_{Kj}N''_{Kj} - N'^2_{Kj}) + qN^2_{Kj}}{2zN_{Kj}N'_{Kj} - qN^2_{Kj}}, \tag{39}$$

$$M_b = \frac{2z^2(N_{Kj}N''_{Kj} - N'^2_{Kj}) + pN^2_{Kj}}{2zN_{Kj}N'_{Kj} - pN^2_{Kj}}, \tag{40}$$

$$M_c = \frac{z(N_{Kj}N''_{Kj} - N'^2_{Kj})}{N_{Kj}N'_{Kj}}, \tag{41}$$

where $N'_{Kj} \equiv \mathrm{d}N_{Kj}/\mathrm{d}z$ and $N''_{Kj} \equiv \mathrm{d}^2N_{Kj}/\mathrm{d}z^2$.

In figure 2 we plot M_c as a function of z for $j = p = q = 0$ and different K. In contrast to the TCS for which mode c remains sub-Poissonian (i.e. $M_c < 0$) in the whole range of z, for KTCSs the mode is super-Poissonian (i.e., $M_c > 0$) at small values of z but then becomes sub-Poissonian when z increases. The crossover point z_{cross} at which the statistics changes from super- to sub-Poissonian moves to the right for higher values of K. At large values of z the mode gets more antibunched in a higher dimension.

For $p > q = 0$ the shape of $M_c = M_a$ appears as in figure 2 but for a fixed K the crossover point z_{cross} shifts to the large-z side with increasing p. For instance, when $K = 3$, numerical calculations give $z_{cross} = 7.5628, 12.0114, 16.3108$ and 20.5606 for $p = 0, 1, 2$ and 3, respectively. Concerning mode b, its behaviour is qualitatively different as displayed in figure 3. In contrast to the TCS for which M_b monotonically increases with z, for KTCSs, it exhibits a maximum which may be located in the super-Poissonian domain if the dimension K is high enough (e.g., if $K \geqslant 4$ when $p = 1$ as illustrated in figure 3(a)). The effect of the charge p is to pull down and right-shift the whole curve (see figure 3(b)) so that for a given K the mode can be made entirely sub-Poissonian (if it was not so) by setting p large enough (see, e.g., figure 3(b) for $K = 4$: $M_b < 0$ in the whole range of z when $p \geqslant 3$).

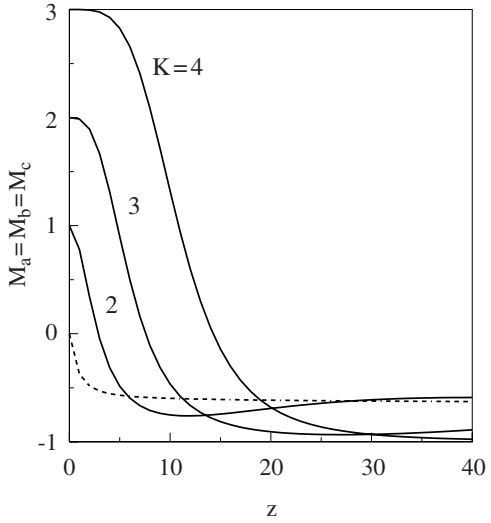

Figure 2. Mandel parameters $M_a = M_b = M_c$ versus $z = r^2$ for $j = p = q = 0$ and different K indicated near the curves. For comparison, the case of TCS (dashed curve) which remains sub-Poissonian in the whole range of z is also plotted.

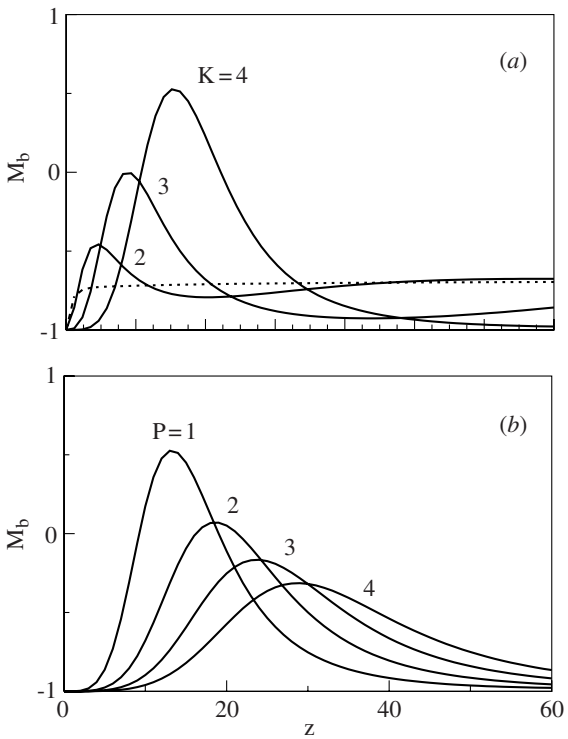

Figure 3. Mandel parameter M_b versus z for $j = q = 0$ while (*a*) $p = 1$ and $K = 2, 3, 4$; (*b*) $K = 4$ and $p = 1, 2, 3, 4$. The dashed curve in (*a*) is the case of TCS which exhibits no maxima.

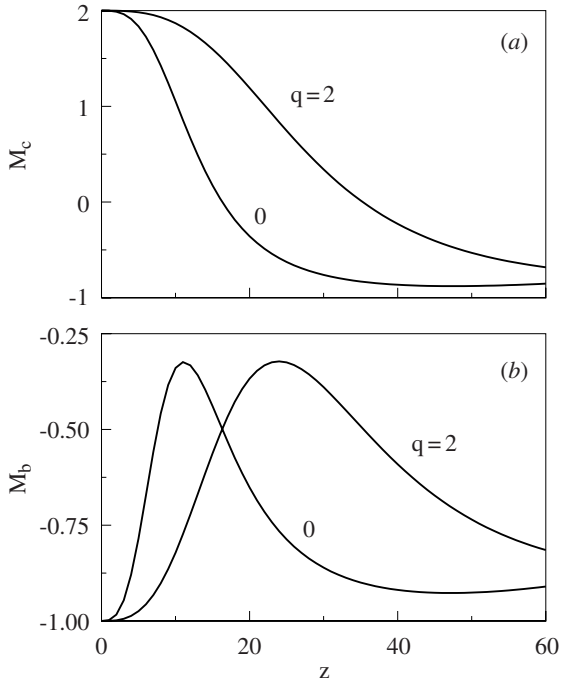

Figure 4. Mandel parameters (*a*) M_c and (*b*) M_b versus z for $K = 3$, $j = 0$, $p = 2$ while $q = 0$ and $q = 2$.

For $p = q > 0$, as mentioned above, $M_a = M_b \neq M_c$. Compared to the situation $p > q = 0$ the following properties hold. For mode c we find the relation $M_c(K, p = q > 0) > M_c(K, p > q = 0)$ in the whole range of z except for $z = 0$ at which $M_c(K, p = q > 0) = M_c(K, p > q = 0)$, as seen from figure 4(*a*). For mode b (*a*) we find that $\max[M_b(K, p = q > 0)] = \max[M_b(K, p > q = 0)]$ but the maximum of $M_b(K, p > q = 0)$ appears 'earlier' than that of $M_b(K, p = q > 0)$ when z is increasing (see figure 4(*b*)).

For $p > 0$, $q > 0$ and $p \neq q$ each mode develops its own dependence on the parameters and is well distinguishable as seen in figure 5.

The specific feature of KTCSs is their degeneracy as explained in section 1. A given manifold characterized by a fixed $K > 1$ consists of K eigenstates enumerated by the parameter $j = 0, 1, 2, \ldots, K-1$. States with the same K but different j differ in their number distribution which is dictated by the Kronecker symbols in equation (33) and by the function $I((n-j)/K)$ in equation (34). This means that one cannot find n quanta of mode c (b, a) in state $|\xi, p, q\rangle_{Kj}$ if $n - j$ ($n - j - p, n - j - q$) is not a multiple of K (see figure 1 for verification). States with the same K but different j differ also in their quantum statistics. So far (in figures 2–5) we have treated only $j = 0$ in which case, for arbitrary K, p and q, we have $M_c(j = 0, z \to 0) \to K-1$ and $M_{a,b}(j = 0, z \to 0) \to -1$. For $j > 0$, however, all three modes are highly antibunched at small values of z independent of K, p and q, i.e., $M_{a,b,c}(j > 0, z \to 0) \to -1$. Also, at small z a state with greater j has a higher degree of antibunching, i.e. its number distribution profile is narrower. These observations are demonstrated in figure 6.

Another intriguing figure of merit is strong correlations between modes of KTCSs. Such correlations are expected to be nonclassical. To verify this we examine the Cauchy–Schwarz

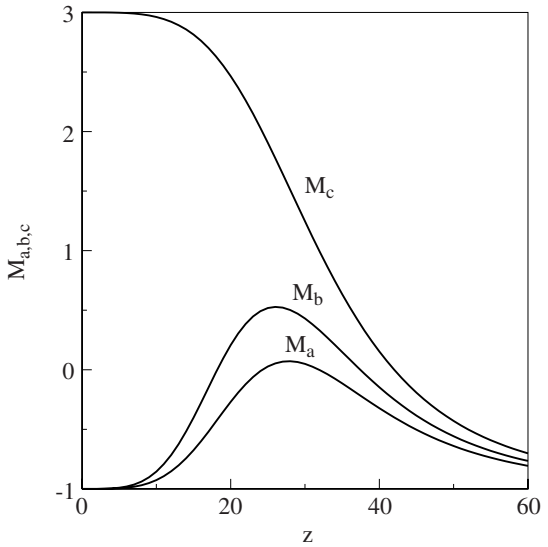

Figure 5. Mandel parameters M_a, M_b and M_c versus z for $K = 4,\ j = 0,\ p = 1$ and $q = 2$.

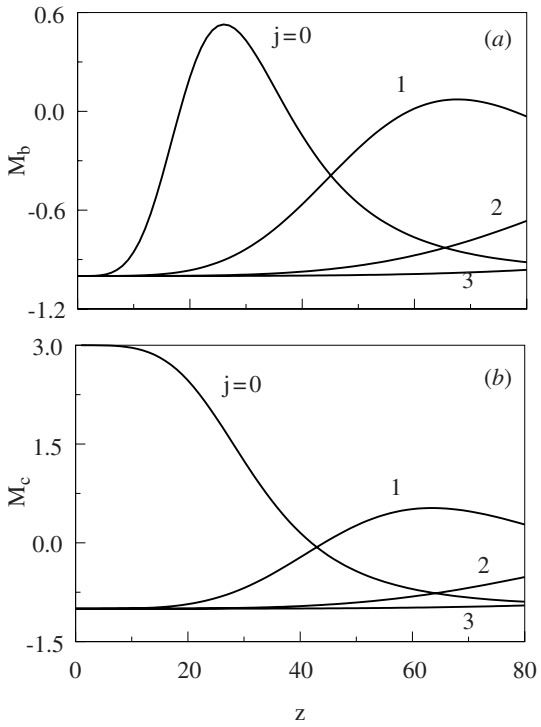

Figure 6. Mandel parameters (*a*) M_b and (*b*) M_c versus z for $K = 4,\ j = 0, 1, 2, 3,\ p = 1$ and $q = 2$.

inequality (CSI) [51] which describes a classical correlation between two modes x and y:

$$J_{xy} = \langle \hat{n}_x^{(2)} \rangle \langle \hat{n}_y^{(2)} \rangle - \langle \hat{n}_x \hat{n}_y \rangle^2 \geqslant 0. \tag{42}$$

General expressions for expectation values of products of two factorial moments $\hat{n}_x^{(l)} \hat{n}_y^{(m)}$ can also be analytically derived for our KTCSs in terms of the normalization coefficient (8). As a result of derivation, we arrive at

$$\langle \hat{n}_a^{(l)} \hat{n}_b^{(m)} \rangle = z^{m-p} N_{Kj}^2 \frac{\mathrm{d}^m}{\mathrm{d}z^m} \left[z^{l+p-q} \frac{\mathrm{d}^l}{\mathrm{d}z^l} \left(\frac{z^q}{N_{Kj}^2} \right) \right], \tag{43}$$

$$\langle \hat{n}_a^{(l)} \hat{n}_c^{(m)} \rangle = z^m N_{Kj}^2 \frac{\mathrm{d}^m}{\mathrm{d}z^m} \left[z^{l-q} \frac{\mathrm{d}^l}{\mathrm{d}z^l} \left(\frac{z^q}{N_{Kj}^2} \right) \right], \tag{44}$$

$$\langle \hat{n}_b^{(l)} \hat{n}_c^{(m)} \rangle = z^{l-p} N_{Kj}^2 \frac{\mathrm{d}^l}{\mathrm{d}z^l} \left[z^{m+p} \frac{\mathrm{d}^m}{\mathrm{d}z^m} \left(\frac{1}{N_{Kj}^2} \right) \right]. \tag{45}$$

Use of (36) and (43)–(45) in (42) yields explicitly

$$\begin{aligned} J_{ab} = N_{Kj}^{-3} \{ & pq(1-p-q) N_{Kj}^3 + 24 z^3 N_{Kj}'^3 \\ & - 2z^2 N_{Kj} N_{Kj}' [(2 + 7(p+q) - (p-q)^2) N_{Kj}' + 4z N_{Kj}''] \\ & + 2z N_{Kj}^2 [6pq N_{Kj}' + z(p+q-(p-q)^2) N_{Kj}'']\}, \end{aligned} \tag{46}$$

$$J_{ac} = 2z^2 N_{Kj}^{-3} \{ 12 z N_{Kj}'^3 + q(1-q) N_{Kj}^2 N_{Kj}'' - N_{Kj} N_{Kj}' [(2 + 7q - q^2) N_{Kj}' + 4z N_{Kj}'']\}, \tag{47}$$

$$J_{bc} = 2z^2 N_{Kj}^{-3} \{ 12 z N_{Kj}'^3 + p(1-p) N_{Kj}^2 N_{Kj}'' - N_{Kj} N_{Kj}' [(2 + 7p - p^2) N_{Kj}' + 4z N_{Kj}'']\}. \tag{48}$$

It is well known that a nonclassical correlation violates the CSI [52], i.e., it makes $J_{xy} < 0$. To assess the degree of CSI violation we scale J_{xy} to $\langle \hat{n}_x \hat{n}_y \rangle^2$, i.e., we use a quantity G_{xy} defined by

$$G_{xy} = \frac{J_{xy}}{\langle \hat{n}_x \hat{n}_y \rangle^2} \tag{49}$$

as a measure of CSI violation. For states with $j > 0$ (i.e., $j = 1, 2, \ldots, K-1$) we find that the CSI is always violated. However, for $j = 0$, although the TCS also always violates the CSI, the KTCSs do not. The violation depends on the type of correlation and the values of charges p, q. The simulation reveals that G_{ab} is always negative but G_{ac} and G_{bc} may be positive depending on the charges. More concretely, when both p and q are not greater than 1 we find that $G_{xy} < 0 \; \forall x, y, K, z$, i.e., the CSI is fully violated. However, when $p\,(q) = 1$ and $q\,(p) \geqslant 2$ the quantity $G_{bc}\,(G_{ac})$ always remains negative but $G_{ac}\,(G_{bc})$ becomes positive at small values of z and the higher the dimension K the wider the z-domain within which the CSI is not violated, i.e., there is a partial violation of the CSI. This behaviour is illustrated in figure 7. Finally, when both $p \geqslant 2$ and $q \geqslant 2$, both the quantities G_{bc} and G_{ac} violate the CSI only partially in the sense mentioned above.

We next study the phase-space characteristics of the KTCSs. For that purpose we consider the three-mode Q-function defined as [53]

$$Q_{\xi pq}^{Kj}(\alpha, \beta, \gamma) = \frac{1}{\pi^3} |_{abc} \langle \alpha, \beta, \gamma | \xi, p, q \rangle_{Kj}|^2, \tag{50}$$

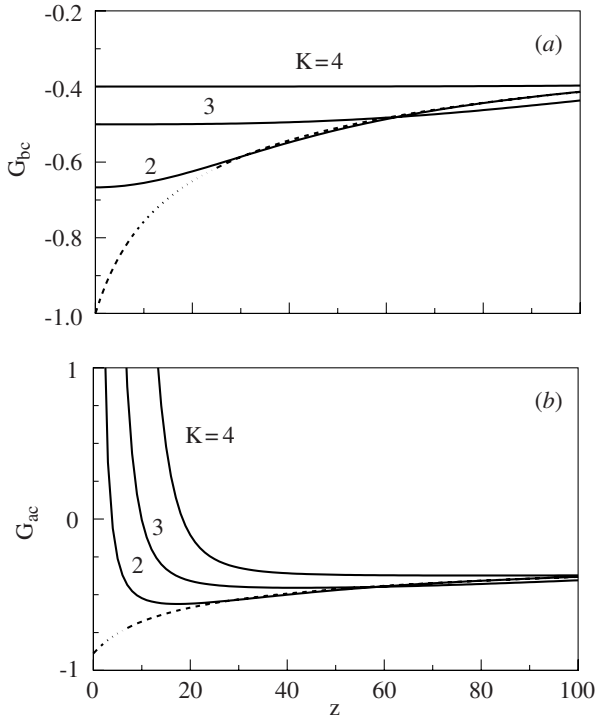

Figure 7. Correlation measures (*a*) G_{bc} and (*b*) G_{ac} versus z for $j = 0, p = 1, q = 2$ and different K as indicated near the curve. For comparison, the case of TCS (dashed curve) which remains negative in the whole range of z is also plotted.

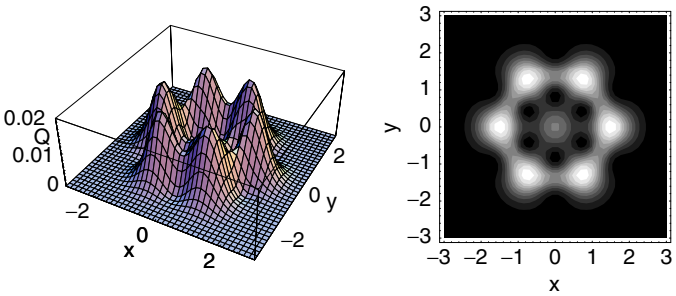

Figure 8. Function $Q = \pi^3 Q^{Kj}_{\xi pq}(x, y)$ and its contour plot for $\xi = 5, p = q = 0, K = 2$ and $j = 0$.

where $\alpha, \beta, \gamma \in \mathcal{C}$ and $|\alpha, \beta, \gamma)_{abc} \equiv |\alpha)_a|\beta)_b|\gamma)_c$ with $|\alpha)_a$, $|\beta)_b$ and $|\gamma)_c$ being the usual coherent states (18) of modes a, b, c, respectively. This function is nonnegative-definite, bounded and normalized to unity

$$\iiint Q^{Kj}_{\xi pq}(\alpha, \beta, \gamma)\, \mathrm{d}^2\alpha\, \mathrm{d}^2\beta\, \mathrm{d}^2\gamma = 1. \tag{51}$$

Generally, there are six variables associated with the real and imaginary parts of α, β and γ. For visualization let us confine ourselves to a subspace determined by $\alpha = \beta = \gamma$. In that

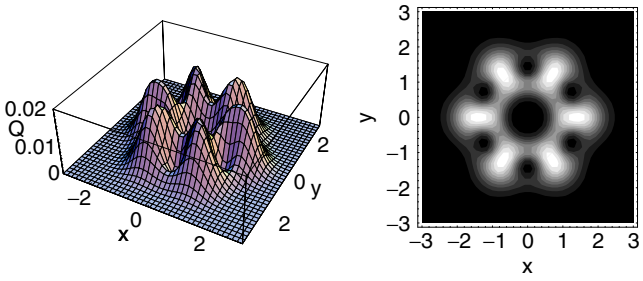

Figure 9. Function $Q = \pi^3 Q^{Kj}_{\xi pq}(x, y)$ and its contour plot for $\xi = 5$, $p = q = 0$, $K = 2$ and $j = 1$.

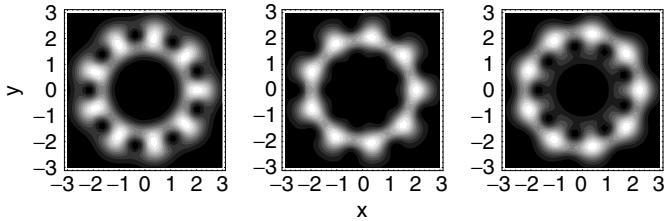

Figure 10. Contour plots of $Q = \pi^3 Q^{Kj}_{\xi pq}(x, y)$ for $\xi = 12$, $p = q = 0$, $K = 3$ with $j = 0$ (left), 1 (middle) and 2 (right).

subspace the Q-function for KTCSs is calculated to be

$$Q^{Kj}_{\xi pq}(x, y) = \frac{1}{\pi^3} N^2_{Kj}(\xi, p, q)\, \mathrm{e}^{-3(x^2+y^2)}(x^2 + y^2)^{p+q} |N^{-2}_{Kj}(\xi(x - \mathrm{i}y)^3, p, q)|^2 \tag{52}$$

with $x = \mathrm{Re}(\alpha)$ and $y = \mathrm{Im}(\alpha)$. We represent in figures 8 and 9 the function $Q^{Kj}_{\xi pq}(x, y)$ and its contour plot for $K = 2$, $j = 0$ and 1. The figures clearly manifest signatures of Schrödinger-cat-like states: constructive (figure 8) and destructive (figure 9) interference fringes between bell-like peaks (there are $3K$ bells for a given K). The $K = 2$ state with $j = 0\,(j = 1)$ is called even (odd) TCS [54, 55]. We also present in figure 10 contour plots for the case of $K = 3$ with $j = 0, 1$ and 2 which shows nine interfering bells. Transparently the pronounced interference fringe structures are j-dependent. It is the phase-space quantum interferences between different TCSs (instead of being simply added) that bring about copious nonclassical signatures of the KTCSs.

4. Physical realization

After having studied physical properties of KTCSs we proceed to find ways to realize them. In this section we are concerned with the context of an ion trap. Since ions can be trapped very efficiently and their entanglement with the environment is extremely weak, trapped ions have advantages for many purposes such as preparing various types of nonclassical states (see, e.g., [56–62]), simulating nonlinear interactions [63], demonstrating quantum phase transitions [64, 65], establishing quantum search algorithms [66], etc. The most promising merit of trapped ion systems is perhaps the possibility of implementing scalable quantum computers [67] in which a number of ions are involved [68–70]. Nevertheless, many tasks can still be done even with a single ion. For instance, a controlled-NOT quantum logic gate can be performed

just by a single trapped ion [71–74]: the target qubit is stored in the ion internal electronic states while the external quantized motional states, i.e., the phonon states, of the same ion serve as the control qubit. Here we propose an experimental scheme to generate KTCSs with $K = 2$ in the vibronic motion of an ion which is trapped in real 3D space. The situations corresponding to 1D and 2D were already considered in [75, 76] for the single- and two-mode cases, respectively.

We first trap a two-level ion of mass M by a 3D isotropic harmonic potential characterized by the trap (phonon) frequency ν. Let $\hat{a}$, $\hat{b}$ and $\hat{c}$ be the phonon annihilation operator in the x-, y- and z-axes, respectively. The ion is then simultaneously driven by 14 travelling-wave lasers (compare with the TCS case [35]) in the resolved sideband regime. The first 13 lasers are all tuned to be resonant with the sixth red motional sideband, i.e., their frequency is $\omega = \Delta - 6\nu$ with Δ being the energy difference between the two electronic levels of the ion. For our purpose it is essential that the lasers be judiciously configured. Namely, we shine the 1st (2nd to 13th) laser along the direction connecting the coordinate origin $\{x, y, z\} = \{0, 0, 0\}$ to a point $\{x, y, z\} = \{1, 1, 1\}$ ($\{1, -1, 1\}$, $\{1, 1, -1\}$, $\{1, -1, -1\}$, $\{1, 1, 0\}$, $\{1, -1, 0\}$, $\{1, 0, 1\}$, $\{1, 0, -1\}$, $\{0, 1, 1\}$, $\{0, 1, -1\}$, $\{1, 0, 0\}$, $\{0, 1, 0\}$ and $\{0, 0, 1\}$). As for the 14th laser, it must be in resonance with the electronic transition, i.e. its frequency is equal to Δ, but its propagation direction is not important. The Hamiltonian of the ion–phonon–laser system is ($\hbar = 1$)

$$H = \frac{\Delta}{2}\sigma_z + \nu(\hat{a}^\dagger\hat{a} + \hat{b}^\dagger\hat{b} + \hat{c}^\dagger\hat{c}) + H_{int}, \tag{53}$$

where

$$H_{int} = \sum_{l=1}^{14} [\Omega_l \exp[-\mathrm{i}(\omega_l t + \varphi_l) + \mathrm{i}\mathbf{k}_l\widehat{\mathbf{R}}_l]\sigma_+ + \mathrm{h.c.}] \tag{54}$$

with Ω_l the Rabi frequencies, $\omega_{1,2,\ldots,13} = \omega$, $\omega_{14} = \Delta$, φ_l are the phases, $\widehat{\mathbf{R}}_l$ is the position operator along the laser direction determined by the wave vector $\mathbf{k}_l$, $\sigma_z = |e\rangle\langle e| - |g\rangle\langle g|$, $\sigma_+ = \sigma_-^\dagger = |e\rangle\langle g|$ and $|g\rangle$ ($|e\rangle$) is the ion's electronic ground (excited) state. Assuming $k_l = k\,\forall l$ there is a single Lamb–Dicke parameter $\eta = k/\sqrt{2M\nu}$ which measures the localization of the ion relative to the laser wavelength. In terms of η we obtain, in an interaction picture with respect to $H_0 = H - H_{int}$, the interaction Hamiltonian of the form

$$\mathcal{H}_{int} = \mathrm{e}^{-\eta^2/2}\sum_{m=0}^{\infty}\frac{(-\eta^2)^m}{m!}\left[-\eta^6\sum_{l=1}^{13}\Omega_l\,\mathrm{e}^{-\mathrm{i}\varphi_l}\frac{(\widehat{A}_l^\dagger)^m\widehat{A}_l^{m+6}}{(m+6)!} + \omega_{14}\,\mathrm{e}^{-\mathrm{i}\varphi_{14}}\frac{(\widehat{A}_{14}^\dagger)^m\widehat{A}_{14}^m}{m!}\right]\sigma_+ + \mathrm{h.c.} \tag{55}$$

In the Lamb–Dicke limit $\eta \ll 1$ we can retain only the $m = 0$ term in (55) and reduce it to

$$\mathcal{H}_{int} = \left[-\frac{\eta^6}{6!}\sum_{l=1}^{13}\Omega_l\,\mathrm{e}^{-\mathrm{i}\varphi_l}\widehat{A}_l^6 + \Omega_{14}\,\mathrm{e}^{-\mathrm{i}\varphi_{14}}\right]\sigma_+ + \mathrm{h.c.} \tag{56}$$

Owing to our configuration for the lasers the operators $\widehat{A}_{1,2,\ldots,13}$ are expressed through $\hat{a}$, $\hat{b}$ and $\hat{c}$ as

$$\widehat{A}_{1,2} = \hat{a} \pm \hat{b} + \hat{c}, \qquad \widehat{A}_{3,4} = \hat{a} \pm \hat{b} - \hat{c}, \tag{57}$$

$$\widehat{A}_{5,6} = \hat{a} \pm \hat{b}, \qquad \widehat{A}_{7,8} = \hat{a} \pm \hat{c}, \qquad \widehat{A}_{9,10} = \hat{b} \pm \hat{c}, \tag{58}$$

$$\widehat{A}_{11} = \hat{a}, \qquad \widehat{A}_{12} = \hat{b}, \qquad \widehat{A}_{13} = \hat{c}. \tag{59}$$

If we control the laser intensities and phases in such a way that

$$\Omega_{1,2,3,4} = \tfrac{1}{2}\Omega_{5,6,7,8,9,10} = \tfrac{1}{4}\omega_{11,12,13} = \Omega, \tag{60}$$

$$\varphi_{1,2,3,4} = \varphi_{11,12,13} = \varphi + \pi, \qquad \varphi_{5,6,7,8,9,10} = \varphi, \qquad \varphi_{14} = \pi, \tag{61}$$

then use of equations (57)–(59) in (56) yields

$$\mathcal{H}_{int} = \zeta[(\hat{a}\hat{b}\hat{c})^2 - \xi^2]\sigma_+ + \text{h.c.}, \tag{62}$$

owing to the identity

$$\sum_{l=1}^{4} \widehat{A}_l^6 - 2\sum_{m=5}^{10} \widehat{A}_m^6 + 4\sum_{n=11}^{13} \widehat{A}_n^6 \equiv 360(\hat{a}\hat{b}\hat{c})^2. \tag{63}$$

The Hamiltonian (62) is the central result for the physical realization under consideration. The new parameters ζ, ξ appearing in (62) are controllable and given simply by

$$\zeta = \frac{\Omega\eta^6}{2}\exp(-\mathrm{i}\varphi), \tag{64}$$

$$\xi^2 = \frac{2\Omega_{14}}{\Omega\eta^6}\exp(\mathrm{i}\varphi). \tag{65}$$

Since the trapped ion is well isolated the dominant channel of decoherence is via the spontaneous decay. Then the time evolution of the system density operator ρ is governed by the following master equation:

$$\frac{\mathrm{d}\rho}{\mathrm{d}t} = -\mathrm{i}[\mathcal{H}_{int}, \rho] + \Gamma\left(\sigma_-\rho\sigma_+ - \frac{\sigma_+\sigma_-\rho}{2} - \frac{\rho\sigma_+\sigma_-}{2}\right), \tag{66}$$

where Γ accounts for the spontaneous decay rate of the ion being in its electronic excited state $|e\rangle$.

It is clear that the system ceases to evolve when the ion's fluorescence stops. Hence, the 'dark' stationary solution of equation (66) in the long-time limit has the ansatz

$$\rho(\infty) = |g\rangle|\Psi\rangle_{xyz}\langle\Psi|\langle g|, \tag{67}$$

where $|\Psi\rangle_{xyz}$ solely determines the phonon state. Setting $\mathrm{d}\rho(\infty)/\mathrm{d}t = 0$ in equation (66) and using properties of the operators $\sigma_\pm$ we arrive at an equation for $|\Psi\rangle_{xyz}$,

$$(\hat{a}\hat{b}\hat{c})^2|\Psi\rangle_{xyz} = \xi^2|\Psi\rangle_{xyz}, \tag{68}$$

where ξ^2 depends on the experiment parameters via (65).

For $|\Psi\rangle_{xyz}$ to be a desired KTCS $|\xi, p, q\rangle_{20}$ or $|\xi, p, q\rangle_{21}$ we need to prepare an appropriate initial state. Furthermore, the generation time is influenced by all the parameters involved. To see these let us simulate equation (66) by the Monte Carlo wavefunction approach [77] with an initial state of the form

$$|\Phi_w(0)\rangle = |e\rangle(\sqrt{w}|\Psi_{l0}\rangle_{xyz} + \sqrt{1-w}|\Psi_{l1}\rangle_{xyz}), \tag{69}$$

where $0 \leqslant w \leqslant 1$ and

$$|\Psi_{lj}\rangle_{xyz} = |2l + q + j\rangle_x|2l + p + j\rangle_y|2l + j\rangle_z \tag{70}$$

with a non-negative integer l and $j = 0$ or 1. Since the dynamics under consideration does not mix the parity, at time $t > 0$ we have

$$|\Phi_w(t)\rangle = \sum_{m=0}^{\infty}(G_m(t)|g\rangle + E_m(t)|e\rangle)(\sqrt{w}|\Psi_{m0}\rangle_{xyz} + \sqrt{1-w}|\Psi_{m1}\rangle_{xyz}), \tag{71}$$

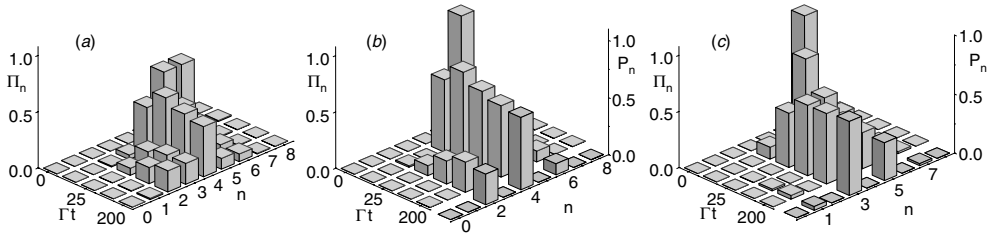

Figure 11. Three-dimensional bar plots of phonon number distribution Π_n at different values of Γt for $\xi = 8$, $p = q = 0$, $\zeta = 0.02$ and $l = 3$. (*a*) $w = 0.5$: no KTCSs are generated since in the long-time limit Π_n is non-zero at both even and odd n, i.e. it does not display the required oscillation. (*b*) $w = 0$: generation of state $|\xi, p, q\rangle_{20}$ is justified in the long-time limit by coincidence of Π_n (equation (72)) with $P_n \equiv P_n(\xi, p, q, 2, 0)$ (equation (34)). (*c*) $w = 1$: generation of state $|\xi, p, q\rangle_{21}$ is justified in the long-time limit by coincidence of Π_n (equation (72)) with $P_n \equiv P_n(\xi, p, q.2, 1)$ (equation (34)).

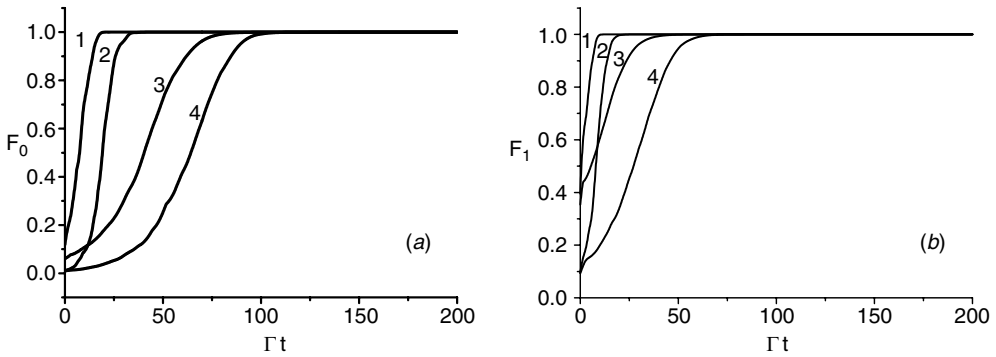

Figure 12. Fidelities (*a*) F_0 and (*b*) F_1 as a function of Γt for different sets of parameters: curves 1, 2, 3 and 4 correspond to $\{\xi, \zeta/\Gamma, p = q, l\} = \{10, 0.005, 2, 0\}$, $\{10, 0.005, 0, 0\}$, $\{6, 0.005, 0, 0\}$ and $\{10, 0.002, 0, 0\}$, respectively.

where G_m and E_m are some time-dependent coefficients to be simulated. In figure 11 we plot the phonon number distribution

$$\Pi_n(t) = |\langle \Phi_w(t)|n + q\rangle_x|n + p\rangle_y|n\rangle_z|^2 \tag{72}$$

at different times. Obviously, for $0 < w < 1$, Π_n may be nonzero at any n. In particular, for $w = 0.5$, there is no oscillation at all in Π_n in the long-time limit (see figure 11(*a*)). Thus, a desired KTCS $|\xi, p, q\rangle_{20}$ or $|\xi, p, q\rangle_{21}$ results only when either $w = 0$ or $w = 1$ as seen from figure 11(*b*) or (*c*). These figures show that in the course of time the phonon number distribution $\Pi_n(t)$ changes gradually and finally tends to coincide with $P_n(\xi, p, q, 2, 0)$ if $w = 0$ (figure 11(*b*)) or with $P_n(\xi, p, q, 2, 1)$ if $w = 1$ (figure 11(*c*)), implying successful generation of the target state $|\xi, p, q\rangle_{20}$ or $|\xi, p, q\rangle_{21}$.

To assess the quality of the resulting state as well as the generation time of our scheme we examine the time dependence of the fidelity

$$F_j(t) = |\langle \Phi_j(t)|\xi, p, q\rangle_{2j}|^2. \tag{73}$$

In figure 12 we represent F_j as a function of Γt for various sets of parameters. Although initially the transient behaviour happens differently for different parameter sets, after some

period of time a stationary regime is inevitably established in all cases. It also follows from the figure that the generation time, i.e., the time needed to reach the stationary regime, is shorter for greater p, q (cf curves 1 and 2), ξ (cf curves 2 and 3) as well as ζ (cf curves 2 and 4). For a wide range of parameters we found that $1 - F_j$ becomes less than 10^{-3} for $\Gamma t \geqslant 200$. The desired KTCS is thus produced with high purity within a relatively short period of time (compared, e.g., with the TCS generation time [35]). The KTCS obtained in our scheme is also stable since its appearance is accompanied by the 'dark' ion which is to be found in the ground state $|g\rangle$ and therefore no longer interacts with the laser fields.

5. Conclusion

We have introduced and studied KTCSs which are both higher-order and multimode. Being a superpositions of phase-correlated TCSs, a KTCS is indeed a new physical state as dictated by the quantum mechanics superposition principle. The novel nonclassical features of KTCSs, as compared to TCSs, were demonstrated in detail and an experimental generation scheme for $K = 2$ was also presented in the ion trap context. Since these KTCSs are entangled states, they promise potential implementations in quantum information processing and quantum computation. In particular, their three-mode nature would be crucial for tasks such as quantum controlled teleportation or/and quantum telecloning of certain types of continuous-variable states as well as inequality-free 'one-shot' tests of local hidden-variable theories, etc. Such applications of KTCSs are in progress and will be reported elsewhere.

Acknowledgments

The authors thank the KIAS Quantum Information Group for useful discussions. HSY was supported by the R&D Program for Fusion Strategy of Advanced Technologies MI-0326-0830002, BAN by KIAS R&D Fund No 03-0149-002 and JK by Korea Research Foundation Grant No KRF-2002-070-C00029.

References

[1] van Loock P and Braunstein S L 2000 *Phys. Rev. Lett.* **84** 3482
[2] Nguyen B A 2003 *Phys. Rev.* A **68** 022321
[3] van Loock P and Braunstein S L 2001 *Phys. Rev. Lett.* **87** 247901
[4] Lynch R 1994 *Phys. Rev.* A **49** 2800
[5] Nguyen B A 2001 *Phys. Lett.* A **284** 72
[6] Truong M D and Nguyen B A 2004 *J. Korean Phys. Soc.* **44** 1421
[7] Nguyen B A and Truong M D 2002 *J. Phys. A: Math. Gen.* **35** 4749
[8] Buzek V, Jex I and Quang T 1990 *J. Mod. Opt.* **37** 159
[9] Sun J, Wang J and Wang C 1992 *Phys. Rev.* A **46** 1700
[10] Jose W D and Mizrahi S S 2000 *J. Opt. B: Quantum Semiclass. Opt.* **2** 306
[11] Liu X M 1999 *J. Phys. A: Math. Gen.* **32** 8685
[12] Nieto M M and Truax D R 2000 *Opt. Commun.* **179** 197
[13] Manko V I, Marmo G, Porzio A, Solimeno S and Zaccaria F 2000 *Phys. Rev.* A **62** 053407
[14] Nguyen B A 2001 *Chinese J. Phys.* **39** 594
[15] Gerry C C and Grobe R 1995 *Phys. Rev.* A **51** 1698
[16] Gou S C, Steinbach J and Knight P L 1996 *Phys. Rev.* A **54** 4315
[17] Liu X M 2001 *Phys. Lett.* A **279** 123
[18] Liu X M 2001 *Phys. Lett.* A **292** 23
[19] Dodonov V V 2002 *J. Opt. B: Quantum Semiclass. Opt.* **4** R1

[20] Hillery M 1989 *Phys. Rev.* A **40** 3147
[21] Nguyen B A and Vo T 1999 *Phys. Lett.* A **261** 34
[22] Nguyen B A and Vo T 2000 *J. Phys. A: Math. Gen.* **33** 2951
[23] Nguyen B A and Vo T 2000 *Phys. Lett.* A **270** 27
[24] Agarwal G S 1986 *Phys. Rev. Lett.* **57** 827
[25] Tara K and Agarwal G S 1994 *Phys. Rev.* A **50** 2870
[26] Gilchrist A, Deuar P and Reid M D 1998 *Phys. Rev. Lett.* **80** 3169
[27] Gilchrist A, Deuar P and Reid M D 1998 *Phys. Rev.* A **60** 4259
[28] Obada A-S F, Abdel-Khalek S and El-Shahat T M 2004 *J. Korean Phys. Soc.* **44** 836
[29] Mancini S and Tombesi P 2003 *Quantum Inform. Comput.* **3** 106
[30] Li S-B, Wu R-K, Wang Q-M and Xu J-B 2004 *Phys. Lett.* A **325** 206
[31] Bhaumik D, Bhaumik K and Dutta-Roy B 1976 *J. Phys. A: Math. Gen.* **9** 1507
[32] Eriksson K E and Skagerstam B S 1979 *J. Phys. A: Math. Gen.* **12** 2175
[33] van Enk S J 2003 *Phys. Rev. Lett.* **91** 017902
[34] Nguyen B A and Truong M D 2002 *J. Opt. B: Quantum Semiclass. Opt.* **4** 80
[35] Yi H S, Nguyen B A and Kim J 2003 *Phys. Lett.* A **315** 6
[36] Sixdeniers J M and Penson K A 2001 *J. Phys. A: Math. Gen.* **34** 2859
[37] Akhiezer N I 1965 *The Classical Moment Problem and Some Related Questions in Analysis* (London: Oliver and Boyd)
[38] Ditkin V A and Prudnikov A P 1965 *Integral Transforms and Operational Calculus* (Oxford: Pergamon)
[39] Sneddon I N 1974 *The Use of Integral Transforms* (New York: McGraw-Hill)
[40] Fernandez D J, Hussin V and Nieto L M 1994 *J. Phys. A: Math. Gen.* **27** 3547
[41] Sixdeniers J M, Penson K A and Solomon A J 1999 *J. Phys. A: Math. Gen.* **32** 7543
[42] Penson K A and Solomon A J 1999 *J. Math. Phys.* **40** 2354
[43] Sixdeniers J M and Penson K A 2000 *J. Phys. A: Math. Gen.* **33** 2907
[44] Klauder J R, Penson K A and Sixdeniers J M 2001 *Phys. Rev.* A **64** 013817
[45] Appl T and Schiller D H 2004 *J. Phys. A: Math. Gen.* **37** 2731
[46] Bender C M and Orszag S A 1978 *Advanced Mathematical Methods for Scientific and Engineers* (Singapore: McGraw-Hill)
[47] Prudnikov A P, Brychkov Yu A and Marichev O I 1990 *More Special Functions* (*Integrals and Series* vol 3) (New York: Gordon and Breach)
[48] Klauder J R 1963 *J. Math. Phys.* **4** 1058
[49] Klauder J R and Skagerstam B S 1985 *Coherent States, Applications in Physics and Mathematical Physics* (Singapore: World Scientific)
[50] Mandel L and Wolf E 1995 *Optical Coherence and Quantum Optics* (Cambridge: Cambridge University Press)
[51] London R 1980 *Rep. Prog. Phys.* **43** 58
[52] Christopher C G and Rainer G 1995 *Phys. Rev.* A **51** 1698
[53] Santos E 2003 *Eur. Phys. J.* D **22** 423
[54] Nguyen B A and Truong M D 2002 *J. Opt. B: Quantum Semiclass. Opt.* **4** 289
[55] Nguyen B A 2003 *Phys. Lett.* A **312** 268
[56] Meekhof D M, Monroe C, King B E, Itano W M and Wineland D J 1996 *Phys. Rev. Lett.* **76** 1796
[57] Monroe C, Meekhof D M, King B E and Wineland D J 1996 *Science* **272** 1131
[58] Munro W J, Milburn G J and Sanders B C 2000 *Phys. Rev.* A **62** 052108
[59] Kis Z, Vogel W and Davidovich L 2001 *Phys. Rev.* A **64** 033401
[60] Solano E, de Matos Filho R L and Zagury N 2001 *Phys. Rev. Lett.* **87** 060402
[61] Solano E, de Matos Filho R L and Zagury N 2002 *J. Opt. B: Quantum Semiclass. Opt.* **4** S324
[62] Nguyen B A and Truong M D 2002 *Int. J. Mod. Phys.* B **16** 519
[63] Milburn G J 1999 *Preprint* quant-ph/9908037
[64] Porras D and Cirac J I 2004 *Preprint* quant-ph/0401102
[65] Barjaktarevic J P, Milburn G J and McKenzie R H 2004 *Preprint* quant-ph/0401137
[66] Agarwal G S, Ariunbold G O, Zanthier J V and Walther H 2004 *Preprint* quant-ph/0401141
[67] Cirac J I and Zoller P 1995 *Phys. Rev. Lett.* **74** 4091
[68] Schmidt-Kaler F, Haffner H, Riebe M, Gulde S, Lancaster G P T, Deuschle T, Becher C, Roos C F, Eschner J and Blatt R 2003 *Nature* **422** 408
[69] Liebfried D *et al* 2003 *Nature* **422** 412
[70] Beige A 2004 *Phys. Rev.* A **69** 012303
[71] Monroe C, Meekhof D M, King B E, Hano W M and Wineland D J 1995 *Phys. Rev. Lett.* **75** 4714
[72] Monroe C, Leibfried D, King B E, Meekhof D M, Itano W M and Wineland D J 1997 *Phys. Rev.* A **55** R2489

[73] Childs A M and Chuang I L 2000 *Phys. Rev.* A **63** 012306
[74] Wei L F and Lei X L 2000 *J. Opt. B: Quantum Semiclass. Opt.* **2** 581
[75] de Matos Filho R L and Vogel W 1996 *Phys. Rev. Lett.* **76** 608
[76] Gou S C, Steinbach J and Knight P L 1996 *Phys. Rev.* A **54** 4315
[77] Dalibard J, Castin Y and Molmer K 1992 *Phys. Rev. Lett.* **68** 580